

Journal of Materials Chemistry A

Materials for energy and sustainability

Accepted Manuscript

This article can be cited before page numbers have been issued, to do this please use: X. Liu, S. Han, Z. Li, S. Ma, Y. Zhi, H. Xia and X. Chen, *J. Mater. Chem. A*, 2020, DOI: 10.1039/D0TA10232F.



This is an Accepted Manuscript, which has been through the Royal Society of Chemistry peer review process and has been accepted for publication.

Accepted Manuscripts are published online shortly after acceptance, before technical editing, formatting and proof reading. Using this free service, authors can make their results available to the community, in citable form, before we publish the edited article. We will replace this Accepted Manuscript with the edited and formatted Advance Article as soon as it is available.

You can find more information about Accepted Manuscripts in the [Information for Authors](#).

Please note that technical editing may introduce minor changes to the text and/or graphics, which may alter content. The journal's standard [Terms & Conditions](#) and the [Ethical guidelines](#) still apply. In no event shall the Royal Society of Chemistry be held responsible for any errors or omissions in this Accepted Manuscript or any consequences arising from the use of any information it contains.

Journal of Materials Chemistry A

Materials for energy and sustainability

Guidelines for Reviewers

Thank you very much for agreeing to review this manuscript for [Journal of Materials Chemistry A](#).



Journal of Materials Chemistry A is a weekly journal in the materials field. The journal is interdisciplinary, publishing work of international significance on all aspects of materials chemistry related to applications in energy and sustainability. Articles cover the fabrication, properties and applications of materials.

Journal of Materials Chemistry A's Impact Factor is **11.301** (2019 Journal Citation Reports®)

The following manuscript has been submitted for consideration as a
FULL PAPER

For acceptance, a Full Paper must report primary research that demonstrates significant **novelty and advance**, either in the chemistry used to produce materials or in the properties/ applications of the materials produced. Work submitted that is outside of these criteria will not usually be considered for publication. The materials should also be related to the theme of energy and sustainability.

When preparing your report, please:

- Focus on the **originality, importance, impact** and **reproducibility** of the science.
- Refer to the **journal scope and expectations**.
- **State clearly** whether you think the article should be accepted or rejected and give detailed comments (with references) both to help the Editor to make a decision on the paper and the authors to improve it.
- **Inform the Editor** if there is a conflict of interest, a significant part of the work you cannot review with confidence or if parts of the work have previously been published.
- **Provide your report rapidly** or inform the Editor if you are unable to do so.

Best regards,

Professor Anders Hagfeldt

Editor-in-Chief
EPFL, Switzerland

Dr Michaela Mühlberg

Executive Editor
Royal Society of Chemistry

Contact us

Please visit our [reviewer hub](#) for further details of our processes, policies and reviewer responsibilities as well as guidance on how to review, or click the links below.





Journal Name

ARTICLE

Bandgap engineering in benzotrithiophene-based conjugated microporous polymers: A strategy for screening metal-free heterogeneous photocatalysts

Songjie Han,^a Ziping Li,^a Si Ma,^a Yongfeng Zhi,^a Hong Xia,^b Xiong Chen,^c and Xiaoming Liu^{*a}Received 00th January 20xx
Accepted 00th January 20xx

DOI: 10.1039/x0xx00000x

www.rsc.org/

Metal-free conjugated microporous polymers (CMPs) as visible-light active and recyclable photocatalysts offer a green and sustainable option to classical metal-based photosensitizers. However, the strategy for screening CMP-based heterogeneous photocatalysts has not been interpreted up to now. Herein, we present a general strategy for obtaining the excellent solid photocatalysts, which is to implement the bandgap engineering in the same series of materials. As a proof of concept, three conjugated porous materials containing benzo[1,2-b:3,4-b':5,6-b'']trithiophene building blocks (BTT-CMP1, BTT-CMP2 and BTT-CMP3) were successfully constructed. They possess permanent porosity with large specific surface area and excellent stability. By changing the linker between benzotrithiophene units, the bandgaps, energy levels and photoelectric performances including absorption, transient photocurrent responses and photocatalytic performances of BTT-CMPs could be handily modulated. Indeed, BTT-CMP2 displayed the best catalytic activity for visible-light-induced synthesis of benzimidazoles in three CMP materials, even higher than that of the small molecule photocatalysts. As a metal-free photocatalyst, interestingly, the screened BTT-CMP2 also showed extensive substrate applicability and outstanding recyclability. Additionally, we hold the opinion that this strategy will prove to be a guiding principle for screening superior CMP-based photocatalysts and broaden their application fields.

Introduction

The exploration and development of semiconductor photosensitizers for the conversion solar energy to chemical energy have turned into one of the most frontier topics of material science owing to the severe energy and environmental challenges.^{1,2} In recent years, a lot of photocatalytic systems have been intensively researched. Despite huge progress in this area, most photocatalysts are short of the basic inherent requirement such as an appropriate optical band gap with optimal frontier electron orbits, effective generation and separation of photogenerated carriers, and outstanding stability. Besides metal-based compounds^{3,4} and organic dyes⁵ often suffer from high price, toxicity and inevitable metal leaching, poor reusability and tedious product purification process, thereby limiting their application in practical purpose. Furthermore, a state-of-art example, graphitic carbon nitride (*g*-C₃N₄)⁶ as classical metal-free organic photocatalysts have

been extensively researched because of its low cost and promising photoelectric properties. In order to increase the visible light absorption and reduce the recombination of photogenerated carriers, however, some modification technologies including doping, copolymerization and dye sensitization are necessary and challenging.^{7,8}

Since the pioneering report by Cooper group in 2007,⁹ conjugated microporous polymers (CMPs) have drawn considerable scientific attentions owing to their wide range of applications as new functional scaffolds.¹⁰⁻¹² The CMPs combine π -conjugated skeleton as well as inherent porosity in one materials, which display fascinating features. The permanent pores offer space for transport, action and transformation of guests, and on the another hand the π -conjugated skeletons ensure effective light absorption, high fluorescence emission, and facilitate exciton migration over the skeleton. Therefore, they have been demonstrated as fluorescent sensing materials.¹³⁻¹⁶ For the first time, the Jiang group used TCB-CMP as a fluorescent molecular sensing device for the detection of explosives with rapid response time and high sensitivity.¹³ Furthermore, recent research reports have still exhibited the underlying applications of CMP materials in heterogeneous photocatalysis such as light-induced hydrogen evolution,¹⁷⁻²² photoinduced degradation of pollutants,²³⁻²⁶ and photocatalytic carbon dioxide reduction.²⁷ More importantly, the photoinduced organic transformations by CMPs are also performance successfully in recent years.²⁸⁻³⁴ Up to now,

^a College of Chemistry, Jilin University, Changchun, 130012, P.R. China.

E-mail: xm_liu@jlu.edu.cn

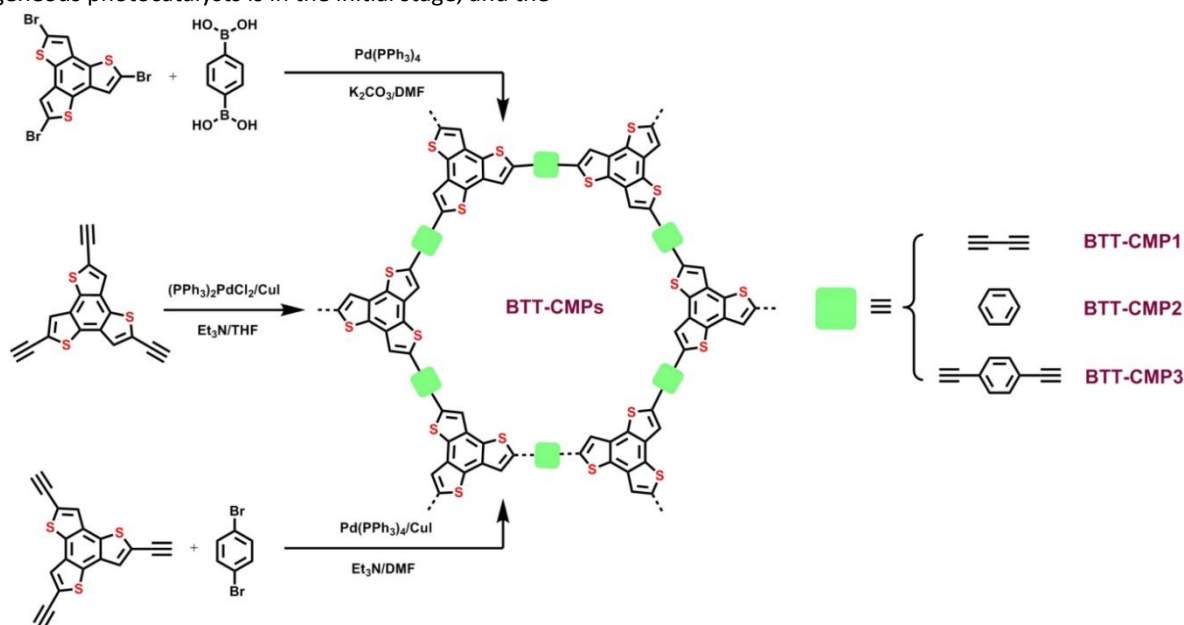
^b State Key Laboratory on Integrated Optoelectronics, College of Electronic Science and Technology, Jilin University, Changchun, 130012, P.R. China.

^c State Key Laboratory of Photocatalysis on Energy and Environment, College of Chemistry, Fuzhou University, Fuzhou, 350002, P.R. China

† Electronic Supplementary Information (ESI) available: Syntheses of monomers and BTT-CMPs, material characterization, general photocatalytic process, and NMR spectra of catalytic products. See DOI: 10.1039/x0xx00000x

nevertheless, the exploration of CMPs as effective heterogeneous photocatalysts is in the initial stage, and the

View Article Online
DOI: 10.1039/D0TA10232F



Scheme 1. (a) Syntheses of BTT-CMPs.

varieties of organic reactions studied are still very limited.²⁹ Meanwhile, the guiding principles for screening of metal-free CMP-based heterogeneous photocatalysts with prominent performances are also rare.

Benzimidazole ring exists widely in biologically active molecules such as many antihypertensive, antiviral, anticancer, antifungal, and psychotropic drugs.^{35,36} Moreover, benzimidazole derivatives are still important intermediates in organic synthesis, auxiliary ligands in transition metal complexes, and are utilized in materials science.³⁷ Hence, the synthesis of benzimidazoles and their derivatives has obtained extensive attraction of chemists for many years. Generally, the currently available methods suffered from the use of hazardous and costly materials, or the requirement for harsh reaction conditions. By comparison, the light-induced synthesis of benzimidazole compounds is a simple, preferably selective, and environment-friendly method.³⁸⁻⁴⁰ Unluckily, the utilized photocatalysts are usually noble metal-based complexes, that set a limit to their application for large-scale experiment in industry.³⁹

In the context, the exploration and development of CMPs as metal-free heterogeneous photocatalysts for the synthesis of new organic reactions are highly expected. We know well that benzo[1,2-b:3,4-b':5,6-b'']trithiophene (BTT) is a fused terthiophene with a sulfur-rich, planar, C_{3h} symmetry and extended π -system, which was widely explored as excellent electron donor units for solar cell.⁴¹ Additionally, the rigid conjugated framework of BTT is appropriate for constructing a porous networks that possess immanent microporosity and prominent physicochemical stability. Indeed, the research of BTT as building block with excellent electron donor property has been extended to the field of organic porous materials.^{42,43} For

example, Jiang group recently reported the BTT-based π -conjugated microporous polymer films through electropolymerization method at the solution-electrode interface.⁴³ Meanwhile, BTT-based porous materials as metal-free heterogeneous photocatalysts are also worth expectation. Taking these factors into account, herein we contribute a general strategy for obtaining the superior metal-free heterogeneous photocatalysts, which is to implement the bandgap engineering in porous polymers. As a proof of concept, three CMP materials containing BTT building blocks (Scheme 1, BTT-CMP1, BTT-CMP2 and BTT-CMP3) were successfully synthesized. By changing the linker between benzotrithiophene units, the bandgap, energy level and photoelectric performances including absorption, transient photocurrent responses as well as photocatalytic activity of BTT-CMPs could be expediently tailored. And screened BTT-CMP2 displayed the best catalytic activity for visible-light-induced synthesis of benzimidazoles in three CMPs, even higher than that of the small molecule photocatalysts. More important, it also showed broad substrate adaptability and outstanding recyclability.

Results and discussion

As manifested in Scheme 1, three BTT-CMPs with the different linkers can be synthesized in high yield by the palladium catalyzed cross-coupling reactions, which are credible processes to prepare CMPs demonstrated by Cooper group. The obtained polymers are fluffy solids, furthermore, it is undissolved in water and general organic solvents. They have good chemical stability, can even resist dilute acid-base solutions. Further, the chemical composition of BTT-CMPs was studied by using Fourier transform infrared (FT-IR), solid-state ¹³C cross-polarized magic angle spin (CP/MAS) nuclear magnetic resonance (NMR) and other spectroscopy and analysis methods.

FT-IR spectra of BTT-CMPs and their monomers were exhibited in Fig. 1a. We found that all CMP

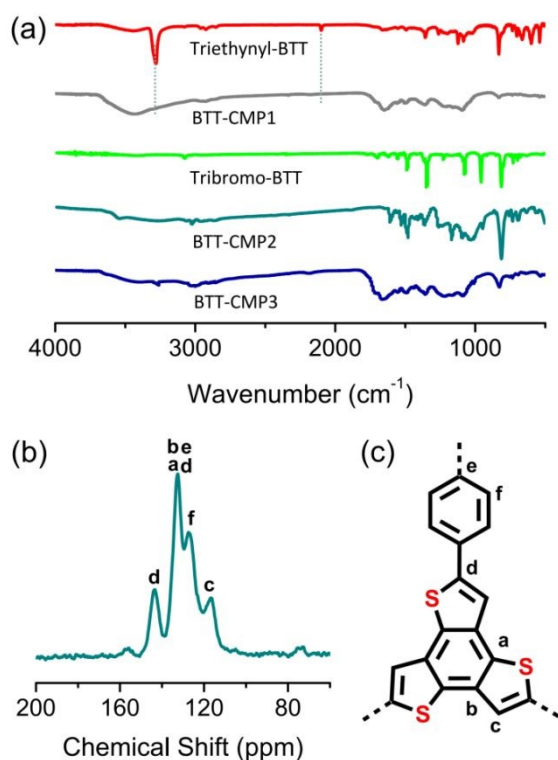


Fig. 1 (a) FT-IR profiles of triethynyl-BTT (red line), BTT-CMP1 (gray line), Tribromo-BTT (green line), BTT-CMP2 (cyan line), and BTT-CMP3 (blue line). (b) Solid-state ¹³C NMR spectrum of BTT-CMP2. (c) The chemical structure of BTT-CMP2.

materials still maintain some characteristic vibration signals of BTT structure, while the broadening features accord with the nature of the polymer. In particular, BTT-CMP1 gives weak broad signals at about 2186 cm⁻¹, which ascribe to the vibration of carbon-carbon triple-bond with disubstituted groups. By

contrast of triethynyl-BTT monomer, however, the signals at 2092 cm⁻¹ for C and 3285 cm⁻¹ for alkyne C-H stretch almost disappeared in FT-IR spectra of BTT-CMP1. These data indicated that the polymerization process is efficient. Furthermore, the chemical structure of BTT-CMPs was contrasted, the broad signals at about 96.5 ppm for BTT-CMP3 can be contributed to alkyne C_{ar}-C≡C-C_{ar} units, and weak peaks at about 78.4 ppm may be from the homocoupling of the alkyne monomer (Fig. S1). The BTT-CMP2 without acetylene units displayed more discrete carbon peaks. The signals at about 143.4 and 116.5 ppm are corresponded to the quaternary and tertiary carbons in thiophene, respectively (Fig. 2b). And resonances at about 132.6 and 126.7 ppm are due to the carbons in phenyl rings. BTT-CMPs did not any signals in powder X-ray diffraction (PXRD) curves, demonstrating that the new materials possess an amorphous character (Fig. S2). As depicted in the field-emission scanning electron microscopy (FE-SEM) images, both materials containing the acetylene units BTT-CMP1 and BTT-CMP3 possessed a band-like morphology at micrometer scale (Fig. S3). For BTT-CMP2, nevertheless, the images revealed that the solid samples are composed of bar-like nanoparticles (Fig. 2a and Fig. S3e). And we can recognize the presence of pores in BTT-CMP2 from high-resolution transmission electron microscopy (HR-TEM) images. (Fig. 2b). In addition, energy-dispersive X-ray spectroscopy (EDS) elemental mapping images clearly showed that the carbon and sulfur elements were distributed uniformly on its skeleton, respectively (Fig. 2c and 2d). The thermal stability of BTT-CMPs was investigated by thermogravimetric analysis (TGA) in a nitrogen atmosphere (Fig. 2e), and 5% mass loss was 300 °C for BTT-CMP1 and BTT-CMP3. In sharp contrast, the thermal decomposition temperature of BTT-CMP2 is as high as 550 °C, indicating it owns a remarkable thermal stability. As depicted in Fig. 2f, the adsorption curves display a sharp nitrogen uptake at relatively low pressure, which proves an inherent

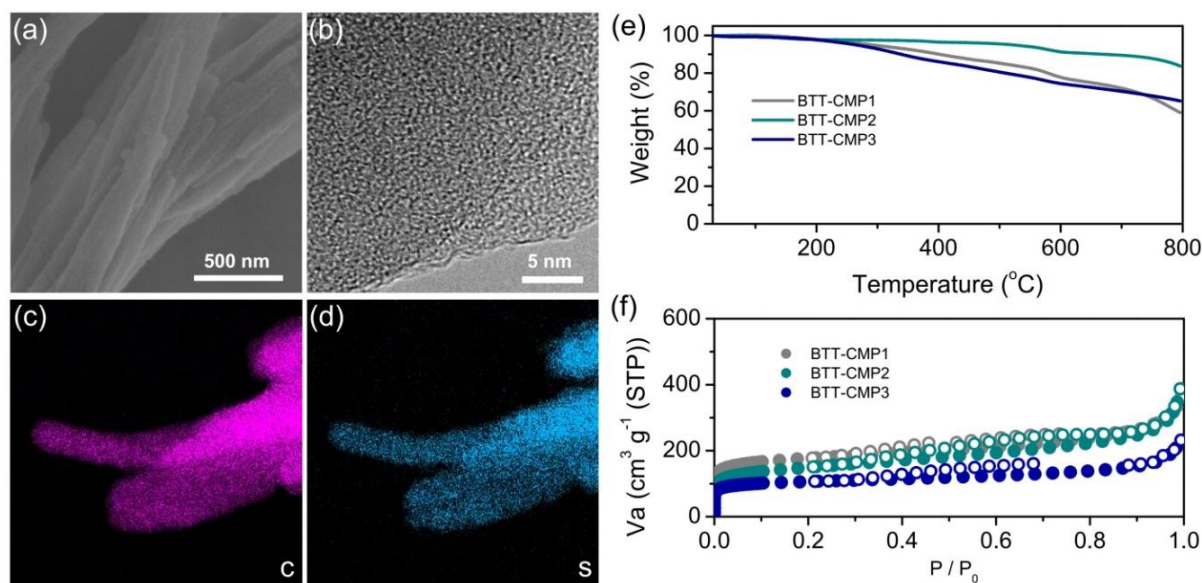


Fig. 2 (a) FE-SEM image (b) HR-TEM image of BTT-CMP2. EDS mapping images of C (c) and S (d) for BTT-CMP2. (e) TGA curves of BTT-CMPs. (f) Nitrogen adsorption-desorption isotherms of BTT-CMPs measured at 77 K (adsorption: filled circle; desorption: open circle).

microporous nature of BTT-CMPs. Based on the nitrogen adsorption data, the Brunauer-Emmett-Teller (BET) surface area was calculated to be $661 \text{ m}^2 \text{ g}^{-1}$, $546 \text{ m}^2 \text{ g}^{-1}$, $404 \text{ m}^2 \text{ g}^{-1}$, which were equivalent to the reported BTT-based DA polymers.⁴² The total pore volume at $p/p_0 = 0.99$ was also evaluated to be $0.563 \text{ cm}^3 \text{ g}^{-1}$ for BTT-CMP1, $0.599 \text{ cm}^3 \text{ g}^{-1}$ for BTT-CMP2 and $0.359 \text{ cm}^3 \text{ g}^{-1}$ for BTT-CMP3, respectively.

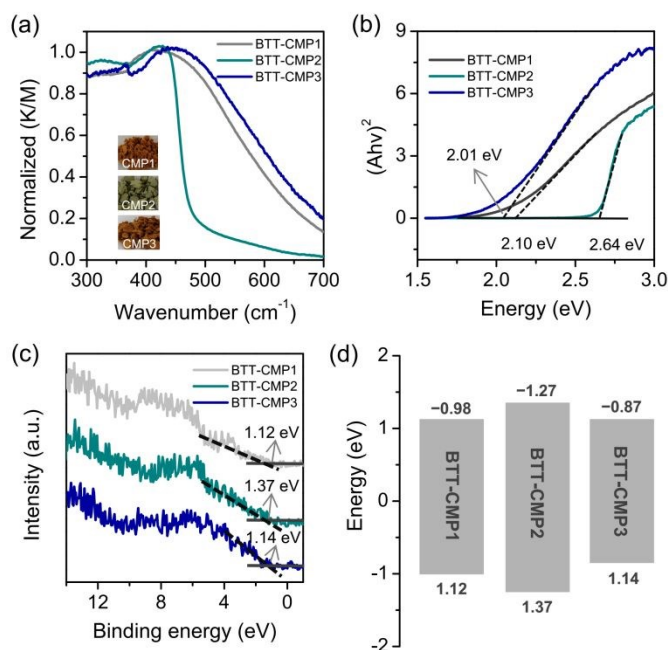
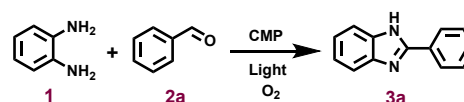


Fig. 3 (a) Solid-state absorption profiles of BTT-CMPs, insets: the corresponding images. (b) Tauc plots of BTT-CMPs. (c) VB-XPS spectra of BTT-CMPs. (d) Schematic diagram of energy band structure about BTT-CMPs and $\text{O}_2/\text{O}_2^{\bullet -}$.

The influence of various linker on the photophysical properties was researched. Firstly, UV/vis diffuse reflectance spectroscopy of all BTT-CMPs were performed. As displayed in Fig. 3a, BTT-CMP2 exhibited an intensive visible-light harvesting with maximum peak at 431 nm (cyan line). In contrast, BTT-CMP1 (gray line) and BTT-CMP3 (blue line) containing the acetylene units showed a broader absorption and the band edge extended to 800 nm. This also corresponds to their color change, from green for BTT-CMP2 to brownish red for BTT-CMP1 and BTT-CMP3 (Fig. 3a, inset). Accordingly, their optical bandgap energy was determined from the corresponding Tauc plot to be 2.10 eV for BTT-CMP1, 2.64 eV for BTT-CMP2 and 2.01 eV for BTT-CMP3, respectively (Fig. 3b). To evaluate the energy

levels of BTT-CMPs, the valence band X-ray photoelectron spectroscopy (VB-XPS) was conducted. The VB edge of BTT-CMP1, BTT-CMP2 and BTT-CMP3 was lied in 1.12 eV, 1.37 eV and 1.14 eV, respectively, as illustrated in Fig. 3c. Taking the VB value from the bandgap energy, therefore, their potential of conduction band (CB) was calculated to be -0.98 eV for BTT-CMP1, -1.27 eV for BTT-CMP2, and -0.87 eV for BTT-CMP3. From Fig. 3d, we can clearly see that the energy band structures of BTT-CMPs can be easily adjusted by changing the linkers. In addition, the potential of CB clearly indicates the reduction of O_2 to $\text{O}_2^{\bullet -}$ (-0.33 eV vs NHE) was realized smoothly through photoinduced electron transfer from BTT-CMPs to O_2 molecule under light illumination. And the driving force of BTT-CMP2 for the electron transfer is larger than that of both BTT-CMPs.

Table 1. Optimization of the photocatalytic conditions for the synthesis of benzimidazole by BTT-CMPs^a



Entry	Catalyst	Solvent	Time (h)	Yield (%) ^a
1	BTT-CMP2	DMF	1	12
2	BTT-CMP2	CH ₃ CN	1	16
3	BTT-CMP2	THF	1	10
4	BTT-CMP2	Toluene	1	14
5	BTT-CMP2	CHCl ₃	1	20
6	BTT-CMP2	CH ₃ OH	1	65
7	BTT-CMP2	Ethanol	1	84
8	~	Ethanol	1	25
9 ^c	BTT-CMP2	Ethanol	1	22
10 ^d	BTT-CMP2	Ethanol	1	63
11 ^e	BTT-CMP2	Ethanol	1	47
12 ^f	BTT-CMP2	Ethanol	1	8
13 ^g	BTT-CMP2	Ethanol	1	70
14 ^h	BTT-CMP2	Ethanol	1	15
15 ⁱ	BTT-CMP2	Ethanol	1	7
16	BTT-CMP1	Ethanol	1	52
17	BTT-CMP3	Ethanol	1	45
18	<i>g</i> -C ₃ N ₄	Ethanol	1	42
19	BTT-CMP2	Ethanol	0.5	38
20	BTT-CMP2	Ethanol	2	91
21	BTT-CMP2	Ethanol	3	93

^aReaction conditions: photocatalyst (3.0 mg), benzaldehyde (0.26 mmol), 1,2-diaminobenzene (0.26 mmol), Oxygen atmosphere (~1.0 atm), 460 nm blue LED lamp with 30 W, 298 K, 60 min. ^bIsolated yield. ^cDark. ^d520 nm green LED lamp with 30 W. ^eWhite LED lamp with 8 W. ^fIn N₂. ^gNaN₃ as the singlet oxygen scavenger. ^hTEMPO as the radical scavenger. ⁱBQ as the superoxide scavenger.

The BTT-CMPs have inherent porosity, excellent stability, moreover, widespread harvesting in visible-light region and good photoredox properties. From the basic principle, these properties satisfied the needs for heterogeneous photocatalysts. Therefore, we utilized the photosynthesis of benzimidazole as a typical reaction to determine the optimal photocatalyst from three BTT-CMPs. And the photocatalytic performance of new CMPs for the synthesis of benzimidazole was investigated, in which *o*-phenylenediamine (**1**), benzaldehyde (**2a**), molecular oxygen were chosen separately as reaction substrates, and eco-friendly oxidant. The effect of different solvents on the reaction yield was first researched. A low yield (10–20%, Table 1, entries 1–5) was procured by BTT-CMP2 in aprotic solvents such as dimethylformamide (DMF), acetonitrile (CH₃CN), tetrahydrofuran (THF), toluene and

chloroform (CHCl₃) under light illumination with a blue LED lamp (30 W, 460 nm). However, methanol (MeOH) proved a general yield under identical reaction criteria (65%, Table 1, entry 6). In sharp contrast, a high yield of 84% was acquired in ethanol (Table 1, entry 7). Besides, the data of control experiments pointed out that photocatalyst BTT-CMP2, light excitation and oxygen gas are all essential for the model reaction (Table 1, entries 8, 9). On the contrary, utilizing a green LED lamp (63%, Table 1, entry 10) or white LED lamp (47%, Table 1, entry 11) as light source, the relatively inferior yields were obtained, respectively. In addition, the photocatalytic process was hardly carried out in nitrogen gas (8%, Table 1, entry 12), demonstrating the critical role of oxygen. It is widely shared that superoxide radical anion (O₂^{•-}) as well as singlet oxygen (¹O₂) as most significant reactive oxygen species play a critical role in the oxybiotic photocatalysis. To ulteriorly explore this photocatalytic mechanism in detail, a sequence of designed experiments were implemented. For example, a ¹O₂ scavenger, sodium azide (NaN₃) was added into the catalytic device, a moderate yield of **3a** was gained (70%, Table 1, entry 13). By contraries, 2,2,6,6-tetramethylpiperidine-1-oxyl (TEMPO) and *p*-benzoquinone (BQ) were injected respectively as radical and O₂^{•-} scavenger in the normative conditions, the yield of product sharply reduced to 15% (Table 1, entry 14) and 7% (Table 1, entry 15). Therefore, these findings manifested that the reactive oxygen species O₂^{•-} is an important intermediate in this photocatalytic reaction. Indeed, the BTT-CMP2 can effectively promote the formation of blue-colored cationic radical and O₂^{•-} upon light illumination, which was mediated through the electron transfer from N,N,N',N'-Tetramethyl-*p*-phenylenediamine (TMPD) to molecular oxygen (Fig. 4a).^{44,45} In addition, the electron paramagnetic resonance (EPR) experiments were conducted in which 5,5-dimethyl-1-pyrroline-N-oxide (DMPO) was used as O₂^{•-} scavenger. We can see clearly from Fig. 4b, the four characteristic peaks corresponding to O₂^{•-} were also observed under light illumination. Based on above observations and previous reports^{38,39,46} for the photosynthesis of benzimidazoles, a possible reaction mechanism is proposed (Fig. 5). First, **1** and **2a** are condensed to form the imine intermediate **I**. Then intramolecular cyclization occurs in **I** to give intermediate **II**. Under light illumination, meanwhile, the photocatalyst generates the excited species BTT-CMP2*, which is reductively quenched by intermediate **II** via a single electron transfer process to obtain intermediate **III** and radical anion BTT-CMP2^{•-}. Subsequently, BTT-CMP2^{•-} is oxidized by molecule oxygen to form O₂^{•-} and regenerate BTT-CMP2. Finally, the target product **3a** was generated through deprotonation and dehydrogenation processes by O₂^{•-} and hydroperoxyl radical HOO*, respectively.

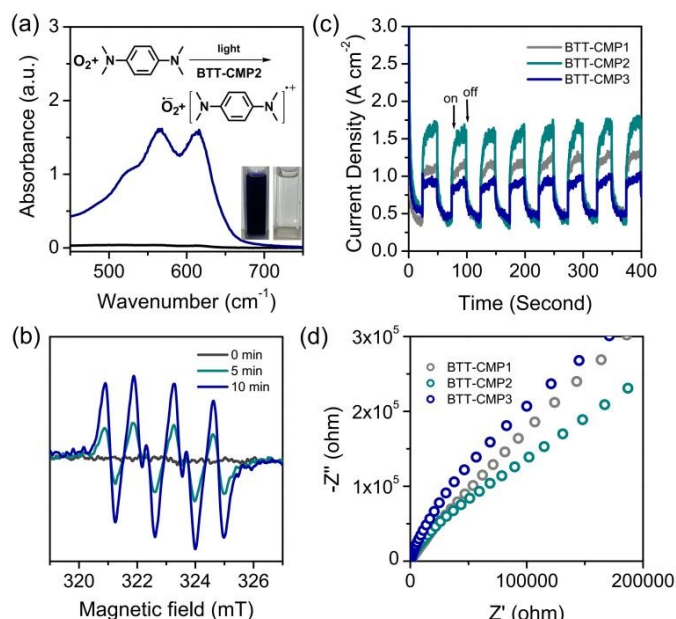


Fig. 4 (a) Absorption profiles of the cationic radical of TMPD generated by BTT-CMP2 under oxygen and light, insets: their corresponding photographs. (b) ESR profiles of BTT-CMP2 (2.0 mg mL^{-1}) and DMPO (0.1 M) in MeOH under light irradiation and dark. (c) Transient photocurrent responses of BTT-CMPs under light irradiation. (d) The EIS Nyquist plots of BTT-CMPs.

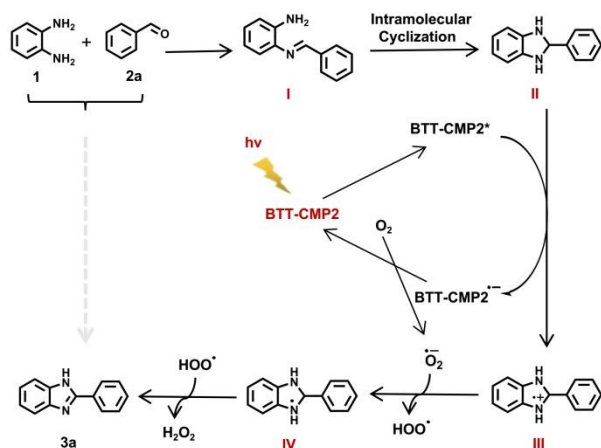


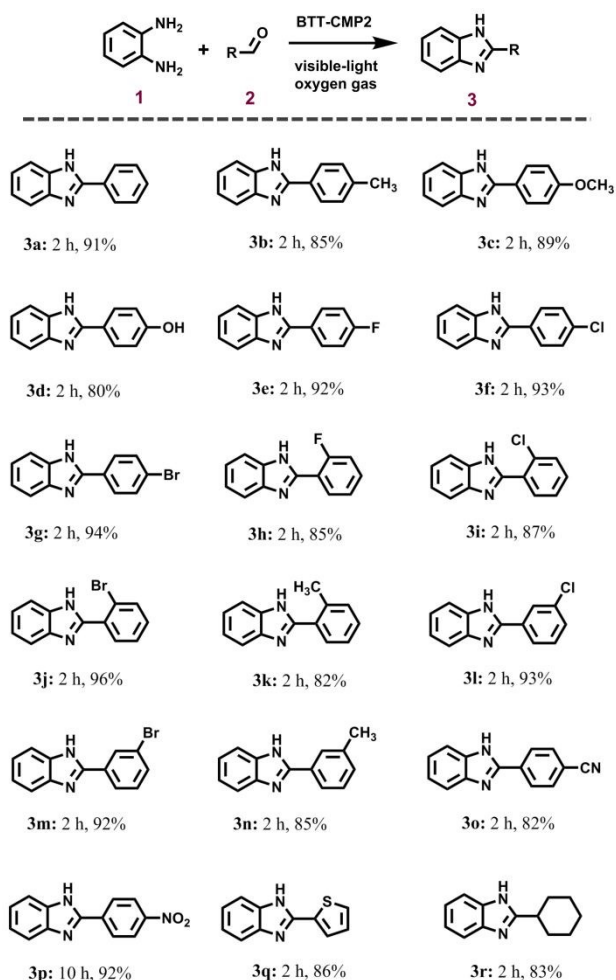
Fig. 5 Proposed mechanism for photosynthesis of benzimidazole in the presence of BTT-CMP2 under visible-light illumination.

In addition, the activity of two polymers BTT-CMP1 and BTT-CMP3 for photosynthesis of benzimidazole was still researched. Interestingly, the reaction gave more moderate yield of 52% for BTT-CMP1 (Table 1, entry 16) and 45% for BTT-CMP3 (Table 1, entry 17) than that of BTT-CMP2 under same conditions, which indicating the significance of linker structure in BTT-CMPs. It is well known that the high-efficient production, separation and transmission of photoinduced charge carrier in photocatalyst network are also essential for enhancing photocatalytic activity. Therefore, we investigated ulteriorly the transient photocurrent response and electrochemical impedance spectroscopy (EIS) of new polymer BTT-CMPs to gain insight into them. Upon visible-light irradiation, all BTT-CMPs displayed rapid photocurrent responses with quite a few reduplicative cycles of intermittent on-off illumination, which gave an

obvious testimony for the photoinduced carries transfer in BTT-CMPs (Fig. 4c). In particular, BTT-CMP2 gave the strongest transient photocurrent in BTT-CMPs, indicating the more effective separation of the photogenerated electron/hole pairs. Additionally, the EIS Nyquist diagram shows that BTT-CMP2 has a smaller radius of arc than the other two BTT-CMPs, demonstrating the charge transfer barrier was decreased with increased charge density in BTT-CMP2 (Fig. 4d). The control experiments indicated that the absorption intensity of blue cationic radical solvents decreased gradually with changing polymer from BTT-CMP2, BTT-CMP1 to BTT-CMP3 (Fig. S4), indicating their similar trend for photogenerated $\text{O}_2^{\bullet-}$ ability. To our delight, it is in good agreement with the photocatalytic activity of BTT-CMPs. Furthermore, the state of art heterogeneous photocatalyst $g\text{-C}_3\text{N}_4$ for this model reaction was also investigated as a comparison with BTT-CMP2. Surprisingly, an inferior yield (42%, Table 1, entry 18) for the target product was gained, indicating the importance of BTT network for photocatalytic activity. Finally, increasing reaction time to 2 h for the model reaction by BTT-CMP2, a superior yield of 91% was gained (Table 1, entry 20). However, the yield increased only slightly when the reaction time was prolonged (Table 1, entry 21). Accordingly, the optimized conditions were determined as: 3.0 mg BTT-CMP2 as the photocatalyst, ethanol as the reaction solvent, oxygen gas as the oxidant, a 30 W blue LED lamp as the light source at $25 \text{ }^\circ\text{C}$ for 2 h.

With screening the optimal photocatalytic conditions, we next researched the photocatalytic benzimidazoles reactions of multifarious aldehydes, such as aromatic and heterocyclic aldehydes as well as cyclic ketone in the presence of BTT-CMP2. As displayed in Table 2, a series of aromatic aldehydes containing diverse electron-donating and electron-withdrawing substituents were effectively transformed to give the corresponding benzimidazole with fine to prominent yields. When benzaldehyde possessed $-\text{F}$, $-\text{Cl}$, $-\text{Br}$, $-\text{CH}_3$, $-\text{OCH}_3$ and $-\text{OH}$ in the p -position (Table 2, 3a–3g), we can find that the yield of product with electron-withdrawing groups is slightly higher than that with electron-rich groups. Similarly, the same trend for the yield of target products was obtained, when the substituent is in the o - and m -positions (Table 2, 3h–3n). In particular, benzimidazole having a nitro group in p -position needs longer reaction time to compared with p -substituted substrates (Table 2, 3p). 2-thiophenylaldehyde as a representative of heterocyclic aldehydes, which transformed into the corresponding benzimidazole with a good yield (Table 2, 3q), suggesting that the photocatalytic system is still suitable for heteroaromatic aldehydes. In addition, this system is also effective for the photosynthesis of benzimidazole with a cycloalkyl group (Table 2, 3r). To our delight, the photocatalytic activity of metal-free BTT-CMP2 is compared with that of the previously reported organic dye and noble metal based polymer.^{38,39}

Table 2. Photocatalytic synthesis of benzimidazoles by BTT-CMP2^o



^aReaction conditions: photocatalyst BTT-CMP2 (3.0 mg), 1,2-diaminobenzene (0.26 mmol), aldehydes (0.26 mmol), ethanol (2.0 mL), oxygen (~1.0 atm), 460 nm blue LED lamp with 30 W, 298.15 K, ^bIsolated yield.

In the heterogeneous reactions, the reusing of the photocatalyst is a prime merit for industrial applications. Therefore, we explored the recovery and recycling of screened BTT-CMP2 as a heterogeneous photocatalyst in synthesis of benzimidazole under visible-light illumination using 1,2-diaminobenzene and benzaldehyde as substrates. The photocatalyst of BTT-CMP2 was facilely separated from the reaction compounds via centrifugation. And the separated BTT-CMP2 was washed with THF and H₂O, dried in reduced pressure, and then utilized the next photocatalytic reaction. We can discover that the BTT-CMP2 can be reused and recycled for 10 cycles without distinct loss of photocatalytic activity (Fig. 6a). It is satisfied that the recovered BTT-CMP2 samples also maintained the original network connectivity (Fig. 5b), aggregated morphology (Fig. 6c and 6d) and large surface area (Fig. 6e, $S_{\text{BET}} = 463 \text{ m}^2 \text{ g}^{-1}$), which is majorly due to its remarkable stability. Finally, we also explored the large scale photosynthesis of BTT-CMP2 using benzaldehyde and 1,2-diaminobenzene as substrates. A marvelous yield of 96% was achieved in the large-scale reaction process, implying its potential application in industrial preparation (Scheme S1).

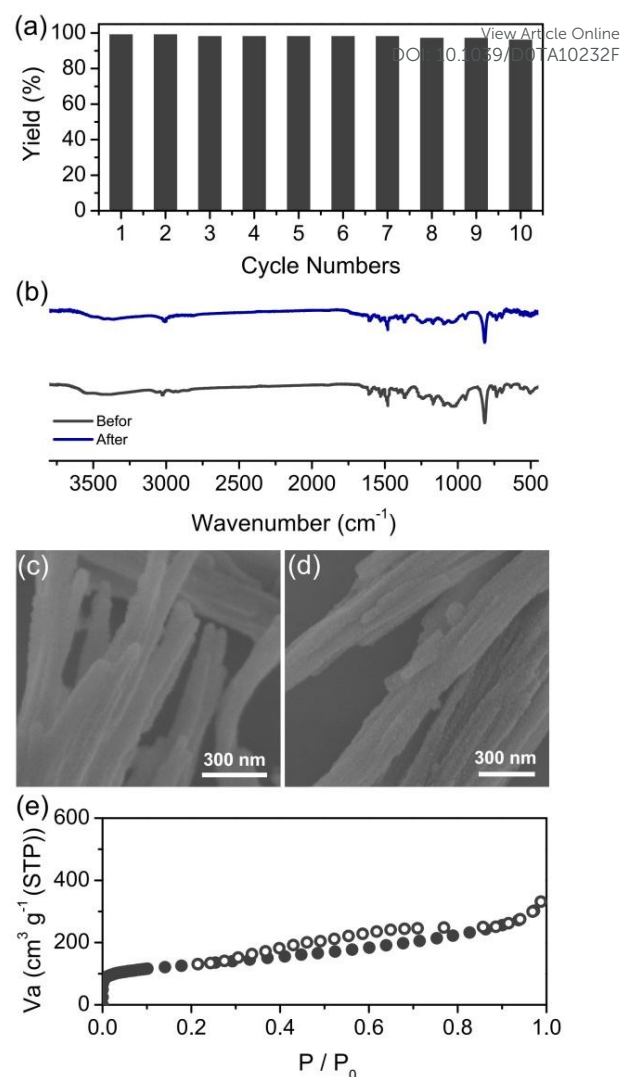


Fig. 6 (a) Reusability of BTT-CMP2 in the photocatalyzing synthesis of benzimidazole of benzaldehyde and 1,2-diaminobenzene. (b) Photocatalyst of BTT-CMP2 first and tenth cycles in FT-IR spectra. FE-SEM images of BTT-CMP2 before (c) and after (d) ten cycles. (e) nitrogen adsorption-desorption choroisotherm (77 K) of BTT-CMP2 after ten cycles ($S_{\text{BET}} = 463 \text{ m}^2 \text{ g}^{-1}$).

Conclusions

In summary, we have donated a strategy for screening CMP-based photocatalysts through the implementation of bandgap engineering. Three benzotrithiophene-based CMPs with various linkers were triumphantly designed and synthesized. The porosity, photoelectric property and energy levels, moreover, bandgaps of obtained CMPs can be easily adjusted by tuning the structure of linkers. Thanks to more effective generation, transfer, separation of the photoinduced carrier and stronger production capacity of O₂^{•-}, BTT-CMP2 has the best catalytic activity for visible-light-induced synthesis of benzimidazoles in three CMP materials, even higher than that of the small molecule photocatalysts and most progressive metal-free photocatalyst *g*-C₃N₄. BTT-CMP2, regarding as a metal-free photocatalyst, not only displayed satisfactory substrate universality, but also showed appreciable recyclability under

visible-light illumination and molecular O₂. We highlight that this work apart from contributes a fresh strategy for screening CMP-based photocatalysts, also broadens the application of CMP materials for sustainable development.

Conflicts of interest

There are no conflicts to declare

Acknowledgements

This work was supported by NSFC (21774040, 52073119 and 21805110).

Notes and references

1. F. Ding, D. Yang, Z. Tong, Y. Nan, Y. Wang, X. Zou, Z. Jiang, *Environ. Sci. Nano*. 2017, **4**, 1455–1469.
2. J. Zhang, Y. Wu, M. Xing, S. A. K. Leghari, S. Sajjad, *Energy Environ. Sci.* 2010, **3**, 715–726.
3. D. M. Schultz, T. P. Yoon, *Science* 2014, **343**, 985.
4. D. A. Nicewicz, D. W. C. MacMillan, *Science* 2008, **322**, 77–80.
5. N. A. Romero, D. A. Nicewicz, *Chem. Rev.* 2016, **116**, 10075–10166.
6. X. Wang, K. Maeda, A. Thomas, K. Takanebe, G. Xin, J. M. Carlsson, K. Domen, M. Antonietti, *Nat. Mater.* 2009, **8**, 76–80.
7. X. C. Wang, S. Blechert, M. Antonietti, *ACS Catal.* 2012, **2**, 1596–1606.
8. D. Masih, Y. Y. Ma, S. Rohani, *Appl. Catal. B: Environ.* 2017, **206**, 556–588.
9. J. X. Jiang, F. Su, A. Trewin, C. D. Wood, N. L. Campbell, H. Niu, C. Dickinson, A. Y. Ganin, M. J. Rosseinsky, Y. Z. Khimiyak, A. I. Cooper, *Angew. Chem. Int. Ed.* 2007, **46**, 8574–8578.
10. A. I. Cooper, *Adv. Mater.* 2009, **21**, 1291–1295.
11. Y. H. Xu, S. B. Jin, H. Xu, A. Nagai, D. L. Jiang, *Chem. Soc. Rev.* 2013, **42**, 8012–8031.
12. A. Thomas, *Angew. Chem. Int. Ed.* 2010, **49**, 8328–8344.
13. X. Liu, Y. Xu, D. Jiang, *J. Am. Chem. Soc.* 2012, **134**, 8738–8741.
14. Y. Zhang, S. A. Y. Zou, X. Luo, Z. Li, H. Xia, X. Liu, Y. Mu, *J. Mater. Chem. A* 2014, **2**, 13422–13430.
15. Z. Li, H. Li, H. Xia, X. Ding, X. Luo, X. Liu, Y. Mu, *Chem. Eur. J.* 2015, **21**, 17355–17362.
16. Y. Zhang, Q. Sun, Z. Li, Y. Zhi, H. Li, Z. Li, H. Xia, X. Liu, *Mater. Chem. Front.* 2020, **4**, 3043–3046.
17. R. S. Sprick, J. X. Jiang, B. Bonillo, S. Ren, T. Ratvijitvech, P. Guiglion, M. A. Zwijnenburg, D. J. Adams, A. I. Cooper, *J. Am. Chem. Soc.* 2015, **137**, 3265–3270.
18. S. Kuecken, A. Acharjya, L. Zhi, M. Schwarze, R. Schomacker, A. Thomas, *Chem. Commun.* 2017, **53**, 5854–5857.
19. S. Bi, Z. Lan, S. Paasch, W. Zhang, Y. He, C. Zhang, F. Liu, D. Wu, X. Zhuang, E. Brunner, X. Wang, F. Zhang, *Adv. Funct. Mater.* 2017, **27**, 1703146.
20. Y. Xu, N. Mao, C. Zhang, X. Wang, J. Zeng, Y. Chen, F. Wang, J. X. Jiang, *Appl. Catal. B: Environ.* 2018, **228**, 1–9.
21. X. Zhang, X. Wang, J. Xiao, S. Wang, D. Huang, X. Ding, Y. Xiang, H. Chen, *J. Catal.* 2017, **350**, 64–71.
22. Z. Lan, W. Ren, X. Chen, Y. Zhang, X. Wang, *Appl. Catal. B: Environ.* 2019, **245**, 596–603.
23. I. Nath, J. Chakraborty, P. M. Heynderickx, F. Verpoort, *Appl. Catal. B: Environ.* 2018, **227**, 102–113.
24. B. Wang, Z. Xie, Y. Li, Z. Yang, L. Chen, *Macromolecules*. 2018, **51**, 3443–3449. DOI: 10.1039/D0TA10232F
25. Y. Li, M. Liu, L. Chen, *J. Mater. Chem. A* 2017, **5**, 13757–13762.
26. W. Ming, S. Bi, Y. Zhang, K. Yu, C. Lu, X. Fu, F. Qiu, P. Liu, Y. Su, F. Zhang, *Adv. Funct. Mater.* 2019, **29**, 1808423.
27. C. Chen, C. Tang, W. Xu, Y. Li and L. Xu, *Phys. Chem. Chem. Phys.* 2018, **20**, 9536–9542.
28. Z. J. Wang, S. Ghasimi, K. Landfester, K. A. I. Zhang, *Adv. Mater.* 2015, **27**, 6265–6270.
29. J. Byun, K. A. I. Zhang, *Mater. Horizons*. 2020, **7**, 15–31.
30. H. P. Liang, Q. Chen, B. H. Han, *ACS Catal.* 2018, **8**, 5313–5322.
31. J. X. Jiang, Y. Li, X. Wu, J. Xiao, D. J. Adams, A. I. Cooper, *Macromolecules* 2013, **46**, 8779–8783.
32. Y. Zhi, K. Li, H. Xia, M. Xue, Y. Mu, X. Liu, *J. Mater. Chem. A* 2017, **5**, 8697–8704.
33. Y. Zhi, S. Ma, H. Xia, Y. Zhang, Z. Shi, Y. Mu, X. Liu, *Appl. Catal. B: Environ.* 2019, **244**, 36–44.
34. Y. Zhi, Z. Yao, W. Jiang, H. Xia, Z. Shi, Y. Mu, X. Liu, *ACS Appl. Mater. Interfaces* 2019, **11**, 37578–37585.
35. K. Tateyama, K. Wada, H. Miura, S. Hosokawa, R. Abe, M. Inoue, *Catal. Sci. Technol.* 2016, **6**, 1677–1684.
36. P. Daw, Y. Ben-David, D. Milstein, *ACS Catalysis*. 2017, **7**, 7456–7460.
37. J. A. Asensio, E. M. Sánchez, P. Gómez-Romero, *Chem. Soc. Rev.* 2010, **39**, 3210.
38. Z. Li, H. Song, R. Guo, M. Zuo, C. Hou, S. Sun, X. He, Z. Sun, W. Chu, *Green Chem.* 2019, **21**, 3602–3605.
39. C. Wang, Y. Han, K. Nie, Y. Li, *Mater. Chem. Front.* 2019, **3**, 1909–1917.
40. C. T. J. Ferguson, N. Huber, T. Kuckhoff, K. A. I. Zhang, K. Landfester, *J. Mater. Chem. A* 2020, **8**, 1072–1076.
41. A. Molina-Ontoria, I. Zimmermann, I. Garcia-Benito, P. Gratia, C. Roldan-Carmona, S. Aghazada, M. Graetzel, M. K. Nazeeruddin, N. Martin, *Angew. Chem. Int. Ed.* 2016, **55**, 6270–6274.
42. Y. S. Kochergin, Y. Noda, R. Kulkarni, K. Škodáková, J. Tarábek, J. Schmidt, M. J. Bojdys, *Macromolecules* 2019, **52**, 7696–7703.
43. C. Gu, N. Huang, Y. Chen, L. Qin, H. Xu, S. Zhang, F. Li, Y. Ma, D. Jiang, *Angew. Chem. Int. Ed.* 2015, **54**, 13594–13598.
44. Z. Li, Y. Zhi, P. Shao, H. Xia, G. Li, X. Feng, X. Chen, Z. Shi, X. Liu, *Appl. Catal. B: Environ.* 2019, **245**, 334–342.
45. Z. Li, S. Han, C. Li, P. Shao, H. Xia, H. Li, X. Chen, X. Feng, X. Liu, *J. Mater. Chem. A* 2020, **8**, 8706–8715.
46. W. An, S. Zheng, Y. Du, S. Ding, Z. Li, S. Jiang, Y. Qin, X. Liu, P. Wei, Z. Cao, M. Song, Z. Pan, *Catal. Sci. Technol.* 2020, **10**, 5171–5180.

A metal-free photocatalyst was screened from the same series of CMP materials through the bandgap engineering strategy. It exhibited excellent photocatalytic performances for synthesis of benzimidazoles with high activity and recyclability.

View Article Online
DOI: 10.1039/D0TA10232F

